Short Communication

CONTRAST MEDIA & MOLECULAR IMAGING

Received: 15 July 2010, Revised: 1 November 2010, Accepted: 2 December 2010, Published online in Wiley Online Library: 2011

(wileyonlinelibrary.com) DOI:10.1002/cmmi.434

The application of ZnO luminescent nanoparticles in labeling mice

Zhan-Yan Pan[a], Jun Liang[a], Zhi-Zhong Zheng[a]*, Huan-Huan Wang[b] and Huan-Ming Xiong[b]*

Photoluminescent ZnO@polymer core–shell nanoparticles were used in mouse imaging through intradermal injections and intravenous injections, and the results proved that such ZnO fluorescence probes are nontoxic to live mice and have great potential in *in vivo* applications. Copyright © 2011 John Wiley & Sons, Ltd.

Supporting information may be found in the online version of this article.

Keywords: ZnO; quantum dots; in vivo

1. Introduction

The applications of photoluminescent semiconductor quantum dots (QDs) in biomedical imaging have gained wide attention in the past decade (1), which has promoted the development of novel diagnostic methods and targeted therapies. Typical QDs based on CdSe and CdTe species have been proved to be poisonous to biological systems, and the synthesis of such materials is harmful to researchers themselves (2). Although various protections employing ZnS, SiO_2, polymers and other nontoxic shells have been developed recently (3), the leakage of Cd ions through the shell defects, the decomposition of nanoparticles by oxygen and the radicals derived from light irradiation are still life-threatening. As a result, scientists are searching for nontoxic substitutes which include nano-scaled ZnSe, InP, carbon, silicon, etc. (4–6). ZnO QD is a promising candidate because it is a cheap, nontoxic photoluminescent semiconductor, but the visible emission of the conventional ZnO QDs does not fit practical requirements. On one hand, the visible emission of the traditional ZnO QDs is rather weak because such emissions arise from ZnO surface defects (7). On the other hand, the conventional ZnO QDs are not stable in water because water can attack the surface luminescent centers and quench ZnO fluorescence immediately (8).

Recently, we synthesized a series of luminescent ZnO@polymer core–shell nanoparticles that were stable in water (9). The polymer shells had two layers, the internal hydrophobic polyester and the outside hydrophilic polyether groups (see Schemes S1 and S2 in the Supporting Information). Such shells made the ZnO nanoparticles soluble in water and prevented the water molecules from destroying ZnO luminescence. For the first time, we applied these ZnO@polymer nanoparticles in live cell imaging using a laser confocal microscope. The ZnO-labeled human cancer cells exhibited bright fluorescence and vivid evolution. Here, we show highly efficient green and yellow emitting ZnO@polymer core–shell nanoparticles in the application of mouse imaging. These QDs are safe for living animals, stable in the circulation and their fluorescence is visible to the naked eye. This is the first report of ZnO QDs applied *in vivo*.

Experimentally, ZnO-1and ZnO-2 QDs were prepared according to the previous method (9). The ethanol solutions of these ZnO@polymer nanoparticles were dialyzed against saline for 3 days to obtain the final aqueous solution containing 0.9 wt% NaCl and 50 mg/ml ZnO nanoparticles. For the imaging study, 3 BALB/ca male nude mice and 27 BALB/c male mice (Shanghai Institute of Materia Medica of Chinese Academy of Science) of 18–22 g at 6–8 weeks of age were used in this study. For intradermal injections, ZnO (0.5 mg in 0.1 ml normal saline) was injected into the left (ZnO-1) and right (ZnO-2) side of the back skin of each BALB/ca nude mouse. For intravenous injection on nine groups of BALB/c mice, doses of 1, 5 and 10 mg in 200 μl normal saline were administered to the mice via the tail vein. Each group of three BALB/c mice was anesthetized prior to sacrifice at different times. All operations on animals were in accord with institutional animal use and care regulations. After intravenous injections, the mice were sacrificed respectively after 5, 30 and 90 min to observe ZnO fluorescence. The whole body images were acquired on a Nikon Coolpix4500 camera, under UV light with the wavelength of 330 nm. The TEM and HRTEM images of ZnO QDs were obtained using a JEM-2010 transmission electron microscope operating at 200 kV.

For the toxicity study, 40 male BALB/c mice (18–22 g at 6–8 weeks of age) were used to evaluate the potential *in vivo* toxicity of ZnO nanoparticles. Mice were housed in steel mesh cages with a 12 h:12 h light:dark illumination cycle and free access to food and water. They were divided into four experimental groups of 10 mice. Doses of 0, 1, 5 and 10 mg ZnO-1 in 200 μl normal saline were administered to on the mice via the tail vein. Functional signs of toxicity, body weight, body temperature and lethality were recorded. Animals were observed after 0, 0.5, 1, 2 and 4 h and just before sacrifice at 24 h after intravenous injections.

* *Correspondence to: H.-M. Xiong or Z.-Z. Zheng*
E-mails: hmxiong@fudan.edu.cn; zhengzhizhong@medmail.com.cn

a *Z.-Y. Pan, J. Liang, Z.-Z. Zheng*
Department of Dermatology of Huashan Hospital, Fudan University, Shanghai 200433, People's Republic of China

b *H.-H. Wang, H.-M. Xiong*
Department of Chemistry and Shanghai Key Laboratory of Molecular Catalysis and Innovative Materials, Fudan University, Shanghai 200433, People's Republic of China

Involuntary movements and SLUD signs (signs of autonomic nervous system disruption including salivation, lacrimation, urination, and defection) were evaluated by the method of Moser and co-workers(10) as described before.(11) Involuntary movements were scored as 2 (normal quivering of vibrissae, head and limbs), 3 (mild, fine tremor typically seen in the forelimbs and head) and 4 (whole body tremor). Autonomic dysfunction was scored as 1 (normal, no excessive secretion), 2 (slight, 1 SLUD sign or very mild multiple signs), 3 (moderate, multiple, overt SLUD signs) and 4 (severe, multiple, extensive SLUD signs). Mice were transferred to metabolic cages through the remainder of the light cycle (about 12 h after the intravenous dosing) for collection of urine and subsequent estimation of urine volume, appearance, color, pH and protein concentration. Blood (about 0.5 ml) was collected via heparinized syringes and centrifuged at 10 000 rpm (1 min) in a microcentrifuge. Plasma was analyzed for blood urea nitrogen (BUN), creatinine, alanine aminotransferase (ALT), total protein, albumin, globulin, alkaline phosphatase and total bilirubin. After collecting blood, mice were euthanized and necropsied. A complete gross and histological necropsy evaluation was performed on all mice. Brain, liver, kidney, lung, heart and spleen were trimmed and fixed in 10% buffered neutral formalin for routine histopathological processing. All data were expressed as 'mean ± standard error' ($X \pm SE$). Statistical significance was determined by one-way analysis of variance (ANOVA) followed by Dunett's multiple comparison test. A value of $p < 0.05$ was considered statistically significant. SPSS software (version 10.0) was used for the statistical analyses.

The TEM image showed that the ZnO@polymer nanoparticles were uniform and monodispersed, and the HRTEM result proved that the particle sizes were 3–4 nm (Fig. 1). Under UV light, ZnO-1 looked green while ZnO-2 appeared yellow. ZnO-1 was brighter than ZnO-2 because ZnO-1 had a quantum yield (QY) of 50% while the QY of ZnO-2 was about 20% (9). The high QY of ZnO aqueous solutions ensured their application in animal imaging. After intradermal injection of QDs, the fluorescence could be clearly seen (Fig. 2) and lasted for more than 90 min. This result indicates that ZnO QDs may be a good probe for imaging skin tissues with the help of *in vivo* fluorescence confocal microscopy or multiphoton microscopy (12), and thus ZnO QDs are useful in the skin carcinoma research (13). However, after intravenous injection, fluorescence from QD was only seen in the vasculature (aorta) and organs (liver and kidney) within 30 min under UV light (Fig. 3 and Table 1). After 90 min, the ZnO fluorescence in the freshly sacrificed mice could not be seen by the naked eye. The intravenous injection experiments suggest that ZnO QDs can be used as a tracker in diseases of vascular malformations and may be helpful in surgery. ZnO luminescence in the circulating blood was not very stable, indicating that the complex blood components could quench ZnO luminescence gradually or that the organs could decompose ZnO QDs. Therefore, to prolong ZnO circulating time in live mice, the ZnO QD surface should be protected more strictly through chemical syntheses.

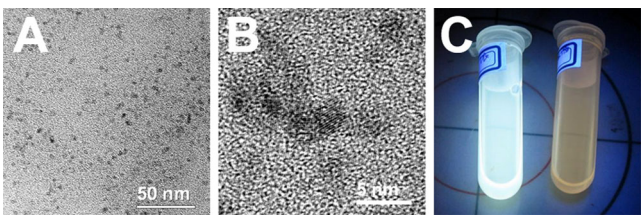

Figure 1. The TEM (A) and HRTEM (B) images of ZnO@polymer nanoparticles. (C) The aqueous solutions of ZnO-1 (left) and ZnO-2 (right) under UV light.

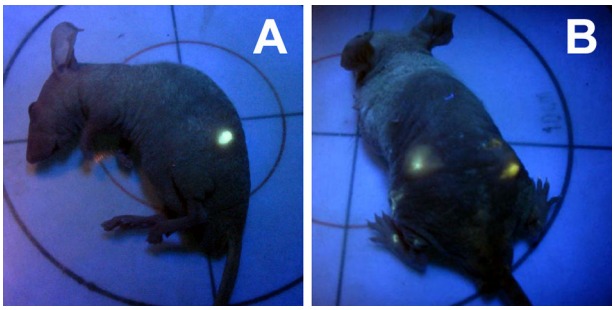

Figure 2. A mouse under UV light after intradermal injection. (A) 5 min after intradermal injection of ZnO-1; (B) 60 min after intradermal injection of ZnO-1 (left side) and ZnO-2 (right side).

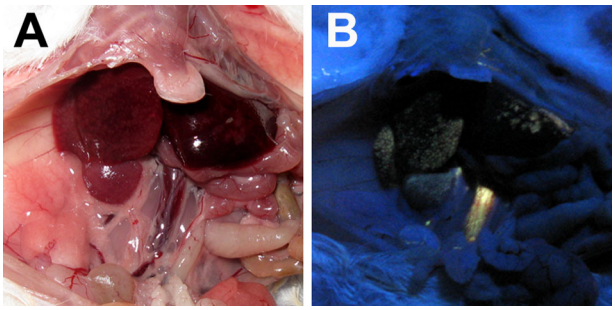

Figure 3. An intravenously injected mouse was sacrificed after 5 min and imaged under (A) daylight and (B) UV light. Note that ZnO-1 nanoparticles locate mainly in the aorta, liver and kidney.

As a highlight of this work, these ZnO@polymer QDs were proved to be nontoxic to live mice. No mice showed obvious intoxication after intradermal injection. Twenty-four hours after treatment, there were no significant differences in body weights between ZnO QD-treated mice and controls (Table S1 in Supporting Information), and the core body temperatures after treatment were not affected (Table S2). No overt signs of toxicity were observed in four groups of mice at any time point. All scores of involuntary movements were 2 and all scores of SLUD signs were 1. There were no significant effects of nanoparticle

Table 1. Number of mice in which fluorescence can be seen by the naked eye at different times. For each test, three mice were used. The intradermal injection employed three mice while the intravenous injection employed 27 mice

	5 min	30 min	90 min
ZnO-1 (left, intradermal)	3	3	3
ZnO-2 (right, intradermal)	3	3	2
ZnO-1 (1 mg, intravenous)	0	0	0
ZnO-1 (5 mg, intravenous)	3	1	0
ZnO-1 (10 mg, intravenous)	3	2	0

Table 2. Effects of ZnO nanoparticles on urinalysis parameters in mice ($n = 10$, $X \pm SE$)[a]

Parameter	Unit	0 mg	1 mg	5 mg	10 mg
Specific gravity	IU/l	1.030 ± 0.01	1.030 ± 0.01	1.030 ± 0.01	1.030 ± 0.01
pH	IU/l	7.4 ± 0.2	7.5 ± 0.5	7.2 ± 0.3	7.5 ± 0.2

[a]Glucose, bilirubin, occult blood and protein were not detected in any samples.

Table 3. Effects of ZnO nanoparticles on plasma chemistry parameters in mice ($n = 10$, $X \pm SE$)

Parameter	Unit	0 mg	1 mg	5 mg	10 mg
Alanine amino transferase	IU/l	78.3 ± 8.1	82.5 ± 5.7	83.2 ± 11.2	89.0 ± 9.4
Aspartate amino transferase	IU/l	95.3 ± 10.7	88.9 ± 5.6	98.5 ± 7.1	97.5 ± 6.2
Total bilirubin	mg/dl	0.20 ± 0.07	0.22 ± 0.10	0.25 ± 0.06	0.24 ± 0.07
Total protein	g/dl	6.3 ± 0.5	6.7 ± 0.8	6.6 ± 1.0	6.8 ± 0.7
Albumin	g/dl	2.27 ± 0.71	2.09 ± 0.35	2.43 ± 0.98	2.11 ± 0.76
Globulin	g/dl	2.35 ± 1.01	2.24 ± 0.82	2.37 ± 0.78	2.22 ± 0.65
Alkaline phosphatase	IU/l	273 ± 15	289 ± 21	299 ± 16	283 ± 19
BUN	mmol/l	13.33 ± 2.2	11.72 ± 1.6	13.85 ± 2.5	14.23 ± 1.7
Creatinine	μmol/l	21.71 ± 3.4	25.1 ± 4.3	22.45 ± 3.7	20.87 ± 2.78

treatment on urinary indicators including protein, glucose, bilirubin or blood cells in the urine, and the specific gravities and pH values were normal (Table 2). Moreover, there were no treatment-related differences in any blood clinical chemistry measurements (Table 3). The routine histopathologic analyses showed no treatment-related histopathological changes in any tissues of the mice. The nontoxic performances of our ZnO QDs are ascribed to their components, i.e. both ZnO itself and the poly(MMA-*co*-PEGMEMA) shells are safe in biological applications. Therefore, the present work proves that ZnO QDs, as safe and cheap luminescent probes, have good prospects for *in vivo* applications.

2. Supporting Information

Supporting information can be found in the online version of this article.

Acknowledgements

This work was supported by the National Natural Science Foundation of China (grant nos 20873029 and 30771953) and Shanghai Committee of Science and Technology (grant no. 09QA1400400).

References

1. Gao XH, Cui YY, Levenson RM, Chung LWK, Nie SM. In vivo cancer targeting and imaging with semiconductor quantum dots. Nat Biotech 2004; 22: 969–976. DOI: 10.1038/nbt994.
2. Pelley JL, Daar AS, Saner MA. State of academic knowledge on toxicity and biological fate of quantum dots. Toxcicol Sci 2009; 112: 276–296. DOI: 10.1093/toxsci/kfp188.
3. Kim BYS, Jiang W, Oreopoulos J, Yip CM, Rutka JT, Chan WCW. Biodegradable quantum dot nanocomposites enable live cell labeling and imaging of cytoplasmic targets. Nano Lett 2008; 8: 3887–3892 ; DOI: 10.1021/nl802311t
4. Gao JH, Chen K, Xie RG, Xie J, Lee S, Cheng Z, Peng XG, Chen XY. Ultrasmall near-infrared non-cadmium quantum dots for in vivo tumor imaging. Small 2010; 6: 256–261. DOI: 10.1002/smll.200901672.
5. Yang ST, Cao L, Luo PG, Lu FS, Wang X, Wang HF, Meziani MJ, Liu YF, Qi G, Sun YP. Carbon dots for optical imaging in vivo. J Am Chem Soc 2009; 131: 11308–11309.
6. Jamieson T, Bakhshi R, Petrova D, Pocock R, Imani M, Seifalian AM. Biological applications of quantum dots. Biomaterials 2007; 28: 4717–4732 . DOI: 10.1016/j.biomaterials.2007.07.014.
7. Xiong HM, Shchukin DG, Möhwald H, Xu Y, Xia YY. Sonochemical synthesis of highly luminescent zinc oxide nanoparticles doped with magnesium(II). Angew Chem Int Edn 2009; 48: 2727.
8. Xiong HM, Wang ZD, Xia YY. Polymerization initiated by inherent free radicals on nanoparticle surfaces: A simple method of obtaining ultrastable (ZnO)polymer core-shell nanoparticles with strong blue fluorescence. Adv Mater 2006; 18: 748–751. DOI: 10.1002/adma.200501899.
9. Xiong HM, Xu Y, Ren QG, Xia YY. Stable aqueous ZnO@polymer core-shell nanoparticles with tunable photoluminescence and their application in cell imaging. J Am Chem Soc 2008; 130: 7522–7523 . DOI: 10.1021/ja800999u.
10. Moser VC, McCormick JP, Creason JP, MacPhail RC. Comparison of chlordimeform and carbaryl using a functional observational battery. Fundam Applic Toxicol 1988; 11: 189–206. DOI: 10.1016/0272-0590(88)90144-3.
11. Liu J, Pope CN. Effects of chlorpyrifos on high-affinity choline uptake and [H-3] hemicholinium-3 binding in rat brain. Fundam. Applic Toxicol 1996; 34: 84–90. DOI: 10.1006/faat.1996.0178.
12. Larson DR, Zipfel WR, Williams RM, Clark SW, Bruchez MP, Wise FW, Webb WW. Water-soluble quantum dots for multiphoton fluorescence imaging in vivo. Science 2003; 300: 1434–1436.
13. Xing Y, Rao JH. Quantum dot bioconjugates for in vitro diagnostics and in vivo imaging. Cancer Biomark. 2008; 4: 307–319.